Acta Geochim (2026) 45:168–184
https://doi.org/10.1007/s11631-025-00794-7

ORIGINAL ARTICLE

Dynamics process of lead-zinc hydrolysis and characterization of its hydrolysis precipitates in a Pb-Zn-NaCl-H_2O system at room temperature and pressure

Junfeng Liu[1] · Yan Zhang[2] · Runsheng Han[2] · Pingtang Wei[3] · Wei Zhu[1]

Received: 28 January 2025 / Revised: 24 April 2025 / Accepted: 22 May 2025 / Published online: 31 July 2025

Abstract Recent studies have confirmed the critical and essential role of elemental hydrolysis in metallogenic processes, such as metal migration and precipitation. However, the kinetic processes, characteristics, and formation mechanisms of hydrolyzed precipitates require further comprehensive investigation. This paper is based on a systematic investigation of the hydrolysis mechanisms of Pb and Zn in various systems under ambient temperature and pressure, the storage conditions of the hydrolyzed precipitates, and the characterization of these precipitates. The results indicate that the hydrolysis behaviors of Pb and Zn exhibit significant differences across various systems. Within the monometallic regime, there is a pronounced disparity in the hydrolysis rates between Pb ions and Zn ions. Pb ions demonstrate a substantially higher degree of hydrolysis, a trend that persists over time and remains largely unaffected by the "fluid retention or isolation" phenomenon in the surrounding environment. Both hydrolytic precipitation rates were observed to decrease in the mixed system, with Zn ions exhibiting less reduction than Pb ions. After hydrolysis, hydrolyzed precipitates can remain in the fluid environment for extended periods of time, which can lead to re-dissolution. Over time, this re-dissolution can increase, eventually leading to significant loss of hydrolyzed precipitates. The hydrolyzed precipitates obtained from the experiments primarily consisted of alkaline carbonates of Pb and Zn. Notably, the crystalline characteristics of the hydrolysis products of Pb and Zn ions exhibited significant differences across various experimental systems; however, the crystallographic characteristics of the primary hydrolysis products are essentially identical to those of their corresponding natural counterparts. Based on the findings from physical phase analysis and previous research, it is concluded that the hydrolysis process consists of three main stages: oxides/hydroxides, carbonates, and alkali carbonates. In the Pb-Zn-NaCl-H_2O system, the proportion of the basic carbonate products of Pb and Zn is 6:2. This research offers an in-depth analysis of the hydrolysis dynamics of lead and zinc under ambient temperature and pressure conditions. Furthermore, it characterizes the crystallization features of the hydrolyzed precipitates and reconstructs the three stages of the formation process. This study holds significant scientific value for understanding the metallogenic mechanisms of Pb and Zn.

Keywords Hydrolysis · Pb-Zn polymetallic mineralization · Hydrolyzed precipitates · Morphological characteristics

✉ Yan Zhang
11301124@kust.edu.cn

✉ Runsheng Han
20190021@kust.edu.cn

Junfeng Liu
mliujunfeng@163.com

Pingtang Wei
373879092@qq.com

Wei Zhu
2972779528@qq.com

[1] Kunming University of Science and Technology, Kunming 650093, China

[2] Southwest Institute of Geological Survey, Geological Survey Center for Nonferrous Metals Resources, Kunming University of Science and Technology, Kunming 650093, China

[3] Kunming Geological Prospecting Institute, China Metallurgical Geological Bureau, Kunming 650024, China

1 Introduction

The mechanisms governing the migration, enrichment, and precipitation of elements during geological evolution constitute a critical component in the mineralization process of ore deposits and are key determinants of both the grade and scale of these deposits (Zhang 1997). Therefore, the investigation into elemental transport and precipitation mechanisms constitutes the foundation for standardizing mineralization processes and elucidating mineralization mechanisms. Deepening the understanding of the ore deposit is instrumental in providing a theoretical foundation for mineral exploration and contributes positively to the advancement of mineralization theory. Currently, alongside theoretical calculations and computer simulations, the primary experimental research methods for investigating the migration and precipitation mechanisms of metallogenic elements are the hydrolysis method and the solubility method. Among these methods, the mineral solubility approach has undergone extensive development and is widely recognized as a standard research tool by scholars both domestically and internationally. This method has yielded significant results in determining the speciation of Pb, Zn, and other elements in hydrothermal fluids, assessing mineral solubility and investigating the dissolution behavior of minerals (Anderson 1973, 1975; Katz and Matthews 1977; Caciagli et al. 2003; Liu et al. 2021; Zhang et al. 2025) and re-precipitation (Zhang et al. 1995; Zhao et al. 2013; Wang et al. 2019). However, it is important to note that the quantity and scale of ion transport in the fluid during elemental migration must be determined based on the stability of the stabilized transport complexes (Baes et al. 1976; Van Baalen 1993). While mineral solubility primarily indicates the quantity of elements that can be leached from the source region, it is insufficient for determining both the number of elements transported within the fluid and the extent of this transport. In contrast to solubility experiments, hydrolysis experiments can comprehensively simulate the dynamic process of elemental migration and enrichment by utilizing metal complexes as research carriers. This approach compensates for the limitations of solubility experiments, which cannot fully capture the changes in complex stability caused by water-rock interactions between metal-ion-rich fluids and surrounding rocks during transport in actual geological evolution. In recent years, hydrolysis experiments have advanced significantly in the fields of metallogenic simulation and theoretical research. He et al. (2015) investigated the stability of fluorotitanium complexes under hydrothermal conditions, thereby obtaining the hydrolysis patterns and reaction constants for these complexes under high-temperature and high-pressure conditions. Zhang et al. (2016) concluded from hydrolysis experiments combined with thermodynamic phase diagrams that pH significantly affects the solubility of galena and sphalerite as well as the complex formation of Pb and Zn. These experiments simulated the critical chemical processes by which Pb and Zn metal ions are hydrolyzed and retained in the ore-holding space during mineralization (Zhang et al. 2019a). Haibo Yan et al. (2020) elucidated the dissolution, migration, and precipitation of platinum group elements (PGE) and the mineralization mechanisms during hydrothermal geological processes by investigating the hydrolysis behavior of PGE-chloride complexes. In conclusion, these studies substantiate the geological significance of elemental hydrolysis in the context of mineralization processes and elucidate the diverse chemical pathways responsible for metal precipitation. The migration of elements from dissolution into the fluid phase, followed by stabilization within the fluid and subsequent precipitation, constitutes a dynamic and protracted process (Van Baalen 1993). Current hydrolysis experiments have primarily focused on the impact of the characteristics of mineralizing hydrothermal fluids on the hydrolysis reaction as well as the influence of the hydrolysis mechanism. However, further research is required to elucidate the specific mechanisms of elemental hydrolysis during the reaction and the influence of other mineralization conditions in the geological environment on the reaction process.

At present, limited research has been conducted on microzonal and microscopic features, including the morphological characteristics of elemental hydrolysis products and mineral crystallization, which are crucial for deducing the mineralization mechanism.

Predecessors have demonstrated the geological significance and dynamic process of Pb-Zn hydrolysis from various perspectives using methods such as hydrolysis experiments, thermodynamic modeling, and computer simulations (Mei et al. 2015; Liu et al. 2018). However, a lack of in-depth research on the characteristics and properties of hydrolysis products remains. This study focuses on the initial metal unloading stage of Pb-Zn ions, thoroughly analyzing the chemical genesis and crystallization processes of Pb-Zn hydrolysis precipitates. It elucidates how these metal precipitates can be preserved in the ore-hosting space over extended periods, awaiting interaction with reductive fluids to facilitate their subsequent transformation into sulfide precipitates. Therefore, building on the findings from previous studies, this paper investigates the hydrolysis dynamics and mechanisms of Pb-Zn hyper-enrichment using Pb-Zn chloride complexes. The study focuses on the chemical composition, mineralogical composition, crystallographic characteristics, and environmental conditions conducive to the long-term stability of Pb and Zn hydrolysis products. It also includes a quantitative analysis and comprehensive comparison of the critical steps and enabling factors in the reaction process, thereby elucidating their underlying mechanisms. By integrating the geological evolution process, this study reconstructs the geochemical pathways of

metal precipitation during the metallogenic evolution of carbonatite-hosted Pb and Zn deposits within a real-world geological framework.

2 Experimental and analytical method

2.1 Principles of hydrolysis and experimental design

Extensive research by numerous scholars (Helgeson 1964; Reed et al. 2006; Yeh et al. 2014) has demonstrated that during the hydrothermal mineralization process, chloro-complexes of Pb and Zn exhibit significantly greater stability at higher temperatures compared to their sulfide complexes. In oxidized, slightly acidic, chlorine-rich, and sulfur-poor fluids, Pb and Zn predominantly exist and migrate as chloro-complexes, primarily in the form of $[PbCl_4]^{2-}$ and $[ZnCl_4]^{2-}$ (Helgeson 1964; Anderson 1975; Reed 2006; Chen et al. 2014, 2015; Yeh et al. 2014; Mei et al. 2015).

Hydrolysis of metal ions is an acid-generating process that primarily involves alterations in H^+ concentration, which is reflected as a change in pH. In reality, hydrolysis of Pb and Zn is widespread in hydrothermal systems, and in the case of Zn, the hydrolysis of the complex anion $[ZnCl_{(4-n)}{}^{n+}]^{2-}$ in hydrothermal fluids proceeds as follows (Zhang et al. 2019a, b):

$$[ZnCl]^+ + H_2O \Leftrightarrow ZnOH^+ + H^+ + Cl^- \quad (1)$$

$$[ZnCl]^0 + 2H_2O \Leftrightarrow Zn(OH)_2 \downarrow + 2H^+3Cl^- \quad (2)$$

$$[ZnCl]_3^- + 3H_2O \Leftrightarrow Zn(OH)_3 + 3H^+3Cl^- \quad (3)$$

$$[ZnCl]_4^{2-} + 4H_2O \Leftrightarrow Zn(OH)_4^{2-} + 4H^+4Cl^- \quad (4)$$

Figure 1 illustrates that under medium-alkaline conditions and at higher ionic activity levels, Zn chloride complexes hydrolyze to form $Zn(OH)_2$ precipitates. This process represents a significant obstacle to Zn transport in hydrothermal fluids. A similar phenomenon is observed for Pb. Hydrolysis experiments of Pb and Zn at ambient temperature and pressure also confirmed that pH = 4 is the threshold for significant hydrolysis of Pb and Zn (Zhang et al. 2019b). Therefore, pH emerges as the paramount control factor in the transport of Pb and Zn.

As illustrated by the aforementioned principles of hydrolysis reactions, the transport phase of Pb and Zn is a dynamic process influenced by multiple factors. To accurately simulate the actual geological processes of mineralization evolution and comprehensively represent all potential processes in the hydrolysis of Pb and Zn, this study designed three reaction systems: Pb-NaCl-H_2O, Zn-NaCl-H_2O and Pb, and Zn-NaCl-H_2O. The experiments were conducted under ambient temperature and pressure conditions. Key variables in this study included time, fluid properties, and water. Based on these considerations, two experimental groups were established: (1) the isolated water group, which is not in contact with the solution after hydrolysis; (2) the retained water group, which remains in contact with the solution after hydrolysis, corresponding to two geological processes:

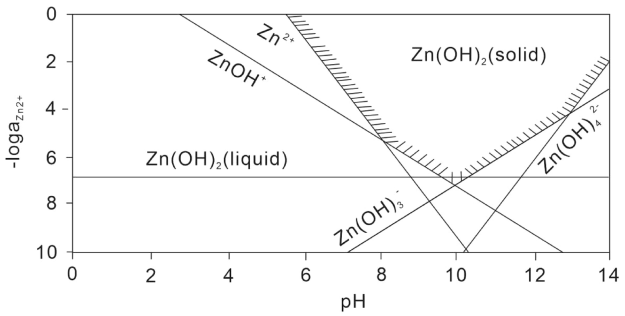

Fig. 1 pH versus log[a(Zn^{2+})] plot, calculated and constructed based on the data from J.A. Dean (1991), as referenced by Zhang et al. (2019a, b)

(a) The acidic mineralizing fluid infiltrates the ore-hosting space, undergoes hydrolysis, releases Pb and Zn mineralized materials, and transports them away from the ore-hosting environment.
(b) The acidic mineralizing fluid infiltrates the ore-hosting space, undergoes hydrolysis, and releases Pb and Zn mineralized materials, but these materials remain within the ore-hosting environment.

To ensure that the two experimental groups exhibited distinct differences, a 13-day experimental period was established following preliminary trials. The sampling interval was set at 24-h intervals, based on previous experimental data (Zhang et al. 2019b).

2.2 Experimental methods

Fluids comprising H_2O, NaCl, and CO_2 are prevalent and significantly influence the evolution of diverse hydrothermal, metamorphic, and igneous environments (Roedder and Bodnar 1997; Touret 2001; Bodnar et al. 2014). In this study, we formulated pertinent solutions by referencing the metal content of the mineralizing fluids from MVT Pb-Zn deposits, for which a more substantial dataset is available (Carpenter et. 1974; Yardley et al. 2005; Stoffell et. 2008; Wilkinson et. 2009). During the preparation of the solution, to ensure that Pb and Zn elements are fully present in the form of complexes, it is essential to stir the solution thoroughly and allow it to stand for a specified duration before proceeding

with subsequent steps. Additionally, acid should be added to adjust the pH to < 4, thereby preventing the hydrolysis of Pb and Zn cations.

2.2.1 Solution formulation

Stock solutions of Na_2PbCl_4, Na_2ZnCl_2, and a mixed Pb–Zn solution were prepared by dissolving analytically pure NaCl, $PbCl_2$, and $ZnCl_2$ in deionized water to achieve final concentrations of $b(PbCl_2) = 0.0010$ mol/L, $b(ZnCl_2) = 0.0152$ mol/L, and $b(NaCl) = 2.0$ mol/L. The solutions were prepared in 1-l volumetric flasks, ensuring complete dissolution and proper mixing.

2.2.2 Hydrolysis experiment setup

Under alkaline to weakly basic conditions, Pb and Zn undergo substantial hydrolysis, resulting in the formation of significant quantities of metal oxide/hydroxide precipitates. Therefore, we elected to promote the hydrolysis of Pb and Zn by adding an appropriate volume of sodium hydroxide (NaOH) solution to the acidic solution. When the pH is > 4, metal ions are hydrolyzed and precipitation occurs, so it is specified that the instantaneous pH in the environment should be maintained between 4 and 4.2 after adding the alkaline solution. Bringing the concentration and volume of solution of the configured alkaline solution and the amount of substance of H^+ corresponding to the upper and lower limits of the desired pH adjustment into the calculation equation (Eq. 5), it can be deduced that the amount of NaOH required to be added ranges from 0.26 to 0.28 ml. To accurately titrate the amount of alkaline solution to prevent causing changes in the volume of the solution before and after titration of the alkaline solution from affecting the final hydrolysis rate calculations, the titration process was carried out using a pipette gun.

2.2.3 Experimental groups

There are six experimental groups in this experiment. The hydrolysis reactions are carried out in a beaker before the reaction by adding dilute hydrochloric acid so that the solution pH is maintained between 3.8 and 4. During the reaction, the Pb and Zn ions in the metal-rich acidic solution configured will react with the hydroxide ions in the dropwise NaOH solution to produce metal hydroxides/oxides. At this time, the environment should be maintained at a pH value between 4 and 4.2. After a day's reaction time, the solution pH is maintained between 5 and 7. Experiments 1 and 2 simulated the effects of the presence or absence of solution on the hydrolysis products under the Pb-NaCl-H_2O system, where Group 1 represented the retained water condition and Group 2 represented the isolated water condition. Experiments 3–4 were conducted in the Zn-NaCl-H_2O system, while experiments 5–6 involved both Pb and the Zn-NaCl-H_2O system. Odd numbered groups (3 and 5) represented the retained water conditions, whereas even numbered groups (4 and 6) represented the isolated water conditions.

(1) **Retained water group**: The hydrolysis of 13 samples was completed on the first day. Following hydrolysis, the resulting precipitates were retained in solution and filtered at 24-h intervals. The precipitates filtered on the first day remained in solution for 24 h, representing the shortest duration, while those filtered on the last day remained in solution for a total of 13 days, which is the longest duration;
(2) **Isolated water group**: Hydrolysis of one sample was conducted daily, followed by immediate filtration and placement in a constant-temperature oven to ensure thorough drying of the precipitates. The initial samples were stored for up to 13 days, while the final processed samples were retained for a minimum of 24 h.

Both experimental groups were established for a 13-day trial period, during which samples were collected at 24-h intervals.

2.2.4 Hydrolysis evaluation

The stability of Pb and Zn complexes under varying conditions and over time can be assessed by evaluating the extent of hydrolysis reactions at ambient temperature and pressure. The parameters that characterize the reaction extent are the hydrolysis rate and the hydrolysis equilibrium constant, where:

$$\text{Hydrolysis ra} = \frac{\text{Initial ion concentration} - \text{Ionic concentration after the reaction}}{\text{Initial ion concentration}} \times 100\%$$

The hydrolysis constant represents the equilibrium constant for the reaction, as indicated in Eq. (5). At low concentrations, the activity coefficient of ions in solution approaches unity, allowing the use of molar concentration in Eq. (5) as a proxy for activity (He et al 2015).

$$K = \frac{c_{H^+}^2}{c_{MeOH^+}} \tag{5}$$

2.2.5 Solid-liquid separation and analysis

The solution obtained after the reaction undergoes solid-liquid separation by first being filtered through qualitative

filter paper, followed by centrifugation at 5000 rpm for 2 min. The resulting supernatant is then transferred to a test tube for further analysis. The precipitate obtained through filtration was transferred to an electrically heated constant-temperature drying oven and dried at 100 °C for 1 h. Subsequently, three successive washes with deionized water were performed to eliminate the interference of rock salt with the reflection signal during testing, The washed samples were subsequently dried and then placed on filter paper, wrapped, and encapsulated in self-sealing bags for testing.

2.3 Analysis methods

The hydrolysis experiments of Pb and Zn solutions in various systems were conducted under ambient temperature and pressure conditions at the High Temperature and High Pressure Laboratory for Rock Formation and Mineralization at Kunming University of Science and Technology. The analytical testing was performed by Guangdong Tuoyan Analytical Testing Co., Ltd. The pH measurements were conducted using a Mettler multiparameter pH meter, which was calibrated on a daily basis at three points with standardized buffer solutions. The specific operation procedures and group arrangements involved in the experiment are shown in Fig. 2.

Following filtration and centrifugation after the reaction of each experimental group, the supernatants were tested at the Analytical Testing Center of Kunming University of Science and Technology using an inductively coupled plasma-optical emission spectrometer (ICP-OES). Scanning electron microscopy analysis equipped with energy-dispersive spectroscopy was carried out. Following carbon plating, SEM images were acquired from regions exhibiting aggregated hydrolysis products (characterized by strong elemental signals) and well-formed crystals compared with reflected light microscopy images. The images were captured in backscattered electron mode, and physical phase analysis of the precipitation samples was obtained after the reaction. The above tests were completed at Guangzhou Tuoyan Inspection Technology Co., Ltd. The test results of x-ray diffraction analysis (XRD) were compared using the ICSD-Mineral (#25,113) database, and the data were analyzed with MDI JADE9 software.

3 Results

3.1 Pb-NaCl-H_2O system

Given that previous researchers (Zhang et al. 2019a, b) have extensively tested the upper clear liquid (Fig. 3), this study focuses on analyzing the hydrolysis products. Therefore, only the treated clear liquid samples from the first and final day (the 13th day) were selected for examination (Table 1). The comparative analysis revealed trends and patterns consistent with prior studies (Zhang et al. 2016).

3.1.1 ICP-OES test results

In the Pb-NaCl-H_2O system, the influence of time on hydrolysis was negligible (as shown in Fig. 4). The hydrolysis rate is > 99%, with a maximum of 99.6%, and the variation over time is within 0.1%. In contrast, in the retained water group where the hydrolysis products remain in solution, a slight redissolution phenomenon is observed; however, this change is not substantial.

3.1.2 SEM and EDS test results

In the Pb-NaCl-H_2O system, most hydrolysis products coalesce to form irregular agglomerates. The size of individual crystal particles is concentrated in the 40–100 μm range, exhibiting morphologies such as microfine grains, needles, and elongated strips (Fig. 7a, b). The primary constituents are hydroxides of Pb and zinc (Zn), with a minor carbonate component (Table 2). Taking RPG-3 as an example, lead oxide (PbO) constitutes its primary component. Among them, Pb is the main element with the highest proportion of 68.25%. It is followed by O with the highest proportion of 31.07% in some areas.

3.1.3 XRD test results

The concentrations of the major components in the submitted samples were quantified using the external standard method, wherein the relative proportions were derived from the intensity ratios of the diffraction lines of the crystalline phases as indicated in the test results. The findings are summarized in Table 3.

Comparing the XRD diffraction patterns of the isolated water group and the retained water group (Fig. 8A, B) shows that both sets of samples exhibit diffractograms characteristic of hydrocerussite [$Pb_3(CO_3)_2(OH)_2$]. Consequently, these samples can be classified as crystalline structures with a defined crystal form. The diffraction intensity of the main peaks for the former sample is approximately 18, while that of the latter sample is < 15. The half-height widths of the two samples are comparable, with the three primary peaks appearing between 24° and 32°. This suggests that both sets of samples share the same compositional makeup. Additionally, the grain size of the samples in the isolated water group is marginally larger than those in the retained water group.

Based on the calculation results (Table 3) and the analysis of the diffraction patterns, in the Pb-NaCl-H_2O system, the primary mineral component of the hydrolysis products is hydrocerussite [$Pb_3(CO_3)_2(OH)_2$]. This compound

Fig. 2 Experimental flow chart

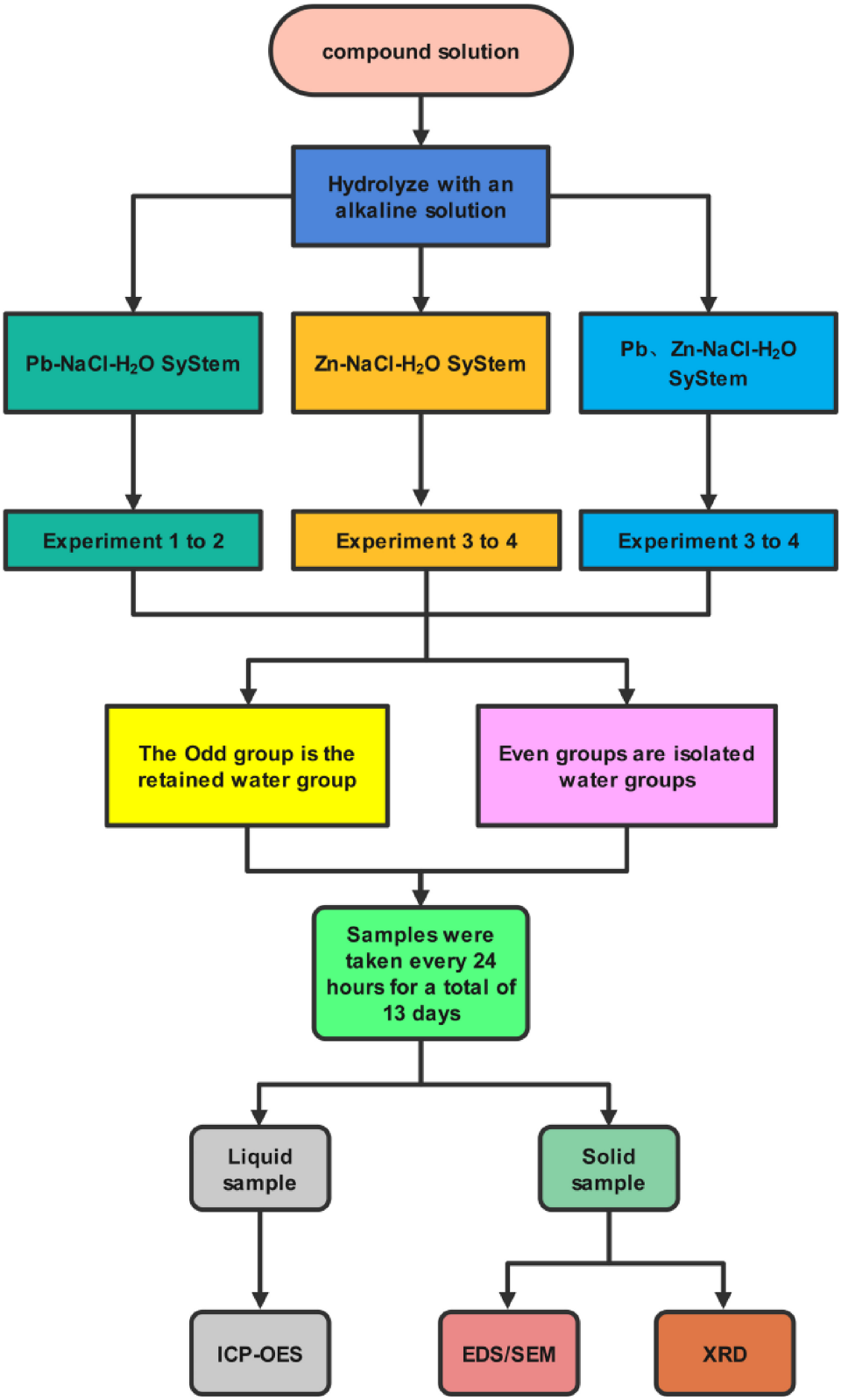

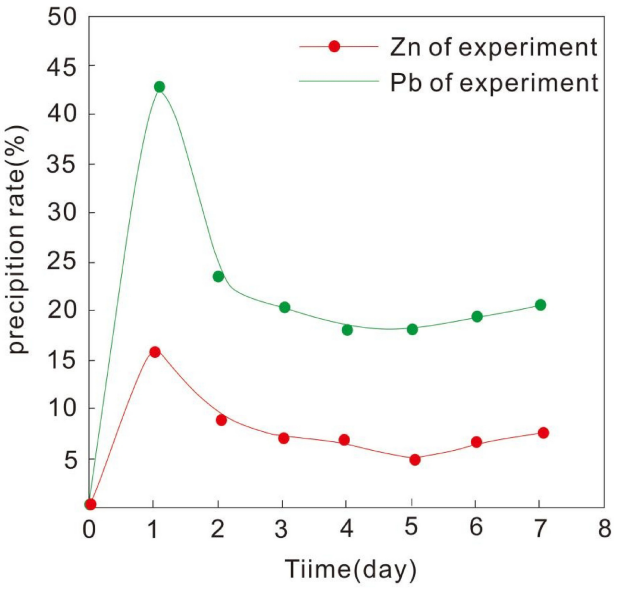

Fig. 3 Pb and Zn ion precipitation rate graphs as referenced by Zhang et al. (2016)

Table 1 ICP-OES results of the clear solution under Pb-NaCl-H_2O system (*Y.* in sample number = acidic solution without alkali drop, *P.* = Pb-NaCl-H_2O system, *Z.* = Zn-NaCl-H_2O system, *R.* = retained water group, *G.* = isolated water group, suffix number. days of experimental time; –. not tested)

System	Number of samples	Test results (mg/L)	
		Pb	Zn
Blank sample	YZP-1	208	1034
	YZ-1	–	1066
	YP-1	211	–
Pb-NaCl-H_2O	RPG-1	1.02	–
	RPG-13	0.67	–
	RPR-1	0.94	–
	RPR-13	1.26	–
Zn-NaCl-H_2O	RZG-1	–	380
	RZG-13	–	527
	RZR-1	–	434
	RZR-13	–	752
Pb-Zn-NaCl-H_2O	RZPG-1	17.09	248
	RZPG-13	56.39	562
	RZPR-1	44.96	466
	RZPR-13	73.21	526

constitutes > 70% of the reaction products in both experimental groups, indicating its dominance under laboratory conditions. Additionally, apart from the unwashed rock salt samples, both groups contain minor amounts of lead carbonate and basic lead chloride compounds, accounting for 2.8%–5.3% and 7.4%–10%, respectively.

3.2 Zn-NaCl-H_2O system

3.2.1 ICP-OES test results

Compared to the hydrolysis extent and precipitate formation trend of Pb ions, Zn ions exhibited significantly lower hydrolysis, with a peak hydrolysis rate of 63.2%. The lowest hydrolysis rate was only 27.2%, with a high variation around 40% (Fig. 5). The hydrolysis of Zn ions was more pronounced in the isolated water group across various environmental conditions, consistent with observations in the Pb-NaCl-H_2O system.

3.2.2 SEM and EDS test results

In the Zn-NaCl-H_2O system, most hydrolysis products aggregate to form irregular prismatic structures. Individual crystal particle sizes are concentrated in the 125–150 μm range and exhibit morphologies such as plate- and scale-like forms (Fig. 7c, d). The primary constituents are hydroxides of lead (Pb) and zinc (Zn), along with minor carbonate components (Table 2). Taking the RZG-13 sample as an example, zinc oxide (ZnO) constitutes its primary component. The highest percentages are Zn, 79.28%, followed by O, up to 30.25% in certain localities.

3.2.3 XRD test results

Comparing the diffractograms of the samples from the two experimental groups showed that the peak intensities of the highest diffraction peaks are relatively similar. However, the isolated water group exhibits a notably higher half-width height and a more pronounced diffraction peak intensity compared to the retained water group. Despite these differences, the distributions of the main diffraction peaks within the diffraction angle range remain highly consistent between the two groups, which indicates that, within the Zn-NaCl-H_2O system, the crystal particle sizes of the hydrolysis products from the isolated water group are significantly larger than those from the retained water group, while the primary chemical compositions remain unchanged.

Based on the XRD test results presented in Table 3 and the diffraction patterns illustrated in Fig. 8C, D, which pertain to the precipitate products from the hydrolysis reaction group, the following analysis is provided: The main

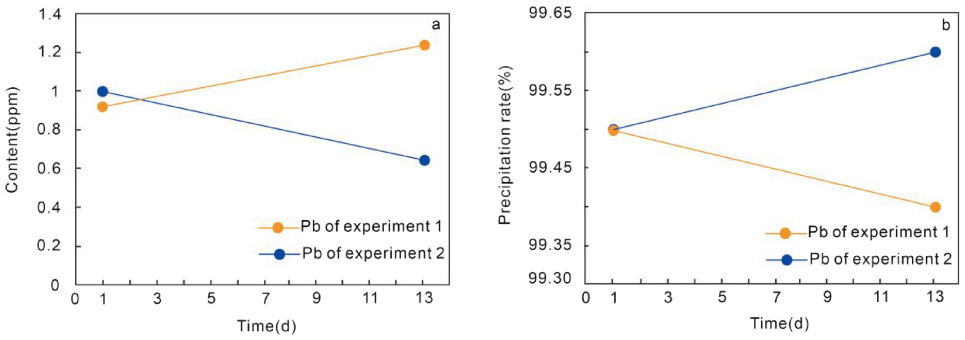

Fig. 4 The graphs depict the metal content in the supernatant (**a**) and the precipitation rate (**b**) following the hydrolysis of the first and second experimental groups

Table 2 EDS point analysis conducted on the hydrolysis precipitate in the Pb-Zn-NaCl-H_2O system

Sample	Point	Element	Weight %	Atomic %	Net Int	Error %	R	A	F
RPG-3	RPG-3-1	PbM	65.25	16.22	8554.65	5.08	0.7782	0.6373	1.0126
		O K	9.76	31.42	715.06	11.67	0.7269	0.0864	1.0000
		NaK	8.14	18.23	1208.70	9.86	0.7452	0.2129	1.0058
		ClK	7.13	10.35	1502.86	7.59	0.7813	0.4541	1.0150
	RPG-3-2	PbM	56.29	10.20	10,954.87	4.95	0.8137	0.6424	1.0070
		O K	31.07	72.88	4382.90	10.22	0.7625	0.1124	1.0000
	RPG-3-3	PbM	65.89	13.44	14,470.56	4.77	0.7867	0.6506	1.0074
		O K	24.09	63.63	3327.95	10.54	0.7352	0.0988	1.0000
	RPG-3-4	PbM	62.57	12.63	12,639.38	4.89	0.7952	0.6409	1.0071
		O K	27.66	72.32	3839.22	10.41	0.7437	0.1063	1.0000
RZG-13	RZG-13-1	ZnK	54.63	22.86	5980.60	2.46	0.9496	0.9863	1.0527
		O K	30.25	45.51	5229.29	10.01	0.8590	0.1250	1.0000
		ClK	4.54	3.50	1946.86	4.93	0.8967	0.6849	1.0169
	RZG-13-2	ZnK	49.39	19.17	6842.71	2.43	0.9535	0.9869	1.0542
		C K	14.14	29.87	637.07	12.23	0.8450	0.0394	1.0000
		O K	28.70	45.51	5229.29	10.01	0.8590	0.1250	1.0000
	RZG-13-3	ZnK	65.36	31.55	6817.07	2.42	0.9407	0.9847	1.0500
		O K	19.32	38.10	2708.60	10.21	0.8341	0.1280	1.0000
	RZG-13-4	ZnK	79.28	48.49	6665.72	2.41	0.9284	0.9827	1.0470
		O K	10.83	27.06	1225.54	10.43	0.8123	0.1284	1.0000
RZPG-13	RZPG-13-1	ZnK	46.20	15.68	3470.65	2.58	0.9563	0.9874	1.0589
		PbM	1.88	0.20	242.32	13.79	0.9058	0.6684	1.0311
		C K	34.58	63.91	1006.25	11.34	0.8510	0.0471	1.0000
		O K	12.30	17.06	880.44	10.95	0.8647	0.0910	1.0000
	RZPG-13-2	ZnK	55.90	25.50	6509.54	2.55	0.9388	0.9812	1.0645
		PbM	6.65	0.96	1220.86	7.00	0.8768	0.6202	1.0288
		O K	12.74	23.75	1619.28	10.61	0.8307	0.1052	1.0000
	RZPG-13-3	ZnK	27.99	11.96	2014.11	3.55	0.9279	0.9700	1.1219
		PbM	28.63	3.86	3253.31	5.22	0.8596	0.6602	1.0147
	RZPG-13-4	ZnK	23.34	9.55	2573.26	3.36	0.9348	0.9723	1.1284
		PbM	26.69	3.45	4708.75	4.97	0.8704	0.6724	1.0146

mineral component in Zn-NaCl-H_2O system is simonkolleite ($Zn_5(OH)_8Cl_2H_2O$), which is also the main mineral formed by the product of the zinc ion hydrolysis reaction under laboratory conditions. The highest percentage reached 72.6%, and the retained water group's value was slightly higher than that of the isolated water group (66.9%), which appeared to have a Zn oxide component of 12.2%.

Table 3 Phase analysis data of hydrolysis products in the NaCl-Pb-Zn-H_2O system under aqueous conditions

Sample	Laurionite (PbCl(OH)	Smithsonite ($ZnCO_3$)	Cerussite ($PbCO_3$)	Zincite (ZnO)	Plattnerite (PbO)	Simonkolleite ($Zn_5(OH)_8Cl_2H_2O$)	Hydrocerussite ($Pb_3(CO_3)_2(OH)_2$)	Rock salt (NaCl)
RPG-3	10%	–	5.3%	–	–	–	71.7%	13%
RPR-3	7.4%	–	2.8%	–	–	–	75.4%	14.4%
RZG-13	–	–	–	12.2%	–	66.9%	–	20.8%
RZR-13	–	–	–	–	–	72.6%	–	27.4%
RZPG-13	–	8.7%	2.5%	4%	7%	56.7%	18%	4.5%
RZPR-13	–	9.6%	2.5%	5.6%	–	51.4%	18.6%	12.4%

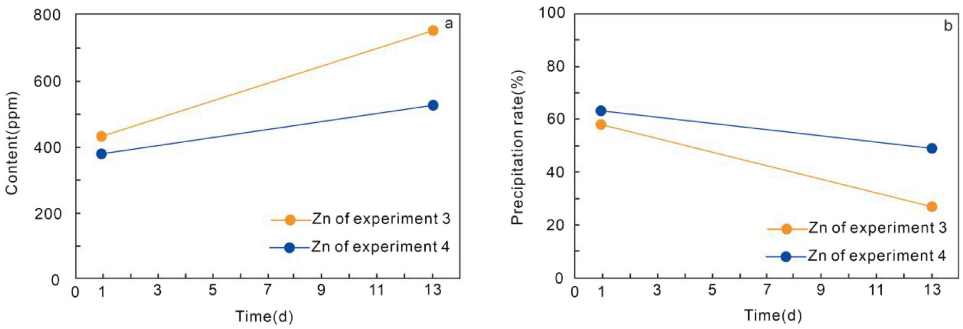

Fig. 5 The graphs depict the metal content in the supernatant (**a**) and the precipitation rate (**b**) following hydrolysis in the third and fourth experimental groups

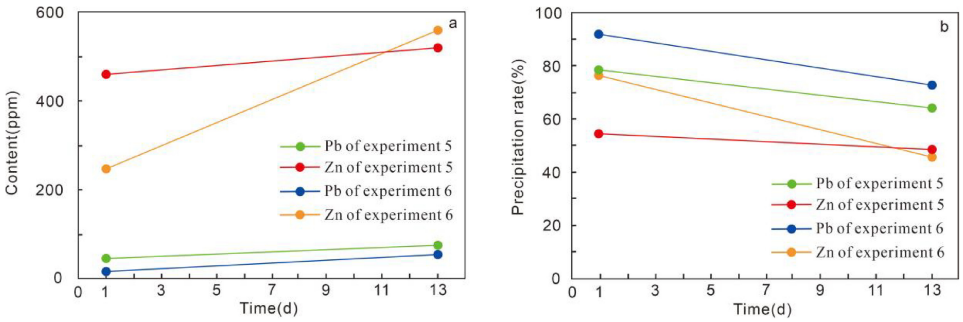

Fig. 6 The graphs depict the metal content in the supernatant (**a**) and the precipitation rate (**b**) following hydrolysis in the fifth and sixth experimental groups

3.3 Pb, Zn-NaCl-H_2O system

3.3.1 ICP-OES test results

Collectively, the extent of hydrolysis of Pb and Zn ions as a function of time shows considerable variation across different systems.

The degree of hydrolysis of metal ions in the isolated water group decreased over time (Fig. 6). Notably, the hydrolysis of Pb ions was less influenced by time progression. The maximum hydrolysis extent reached 91.7%, but the hydrolysis rate on the final day (72.8%) was the lowest. Overall, the trend in the degree of hydrolysis for Pb ions remained relatively stable. The hydrolysis rate of Zn ions is higher than that of Zn-NaCl-H_2O (with the maximum precipitation rate reaching 76%), but the difference in the lowest hydrolysis rate is not significant over time (45.6%).

The hydrolysis rates of the two metal ions in the retained water group exhibited a decreasing trend over time. Notably, the maximum hydrolysis rate of Pb ions was significantly lower (only 78.3%) compared to that in the isolation water group. However, the rate of decrease slowed over time, with the minimum hydrolysis rate reaching 64.8%. On the other hand, the hydrolysis behavior of Zn ions exhibited a significant decrease in maximum hydrolysis rate from 76% to 54.9%. Similar to Pb ions, the trend in the hydrolysis rate of Zn ions also showed a marked deceleration, with the lowest observed hydrolysis rate being 49.1%, marginally higher than that of the control group.

3.3.2 SEM and EDS test results

In the Pb-Zn-NaCl-H_2O system, the precipitates formed during hydrolysis experiments predominantly coalesced into

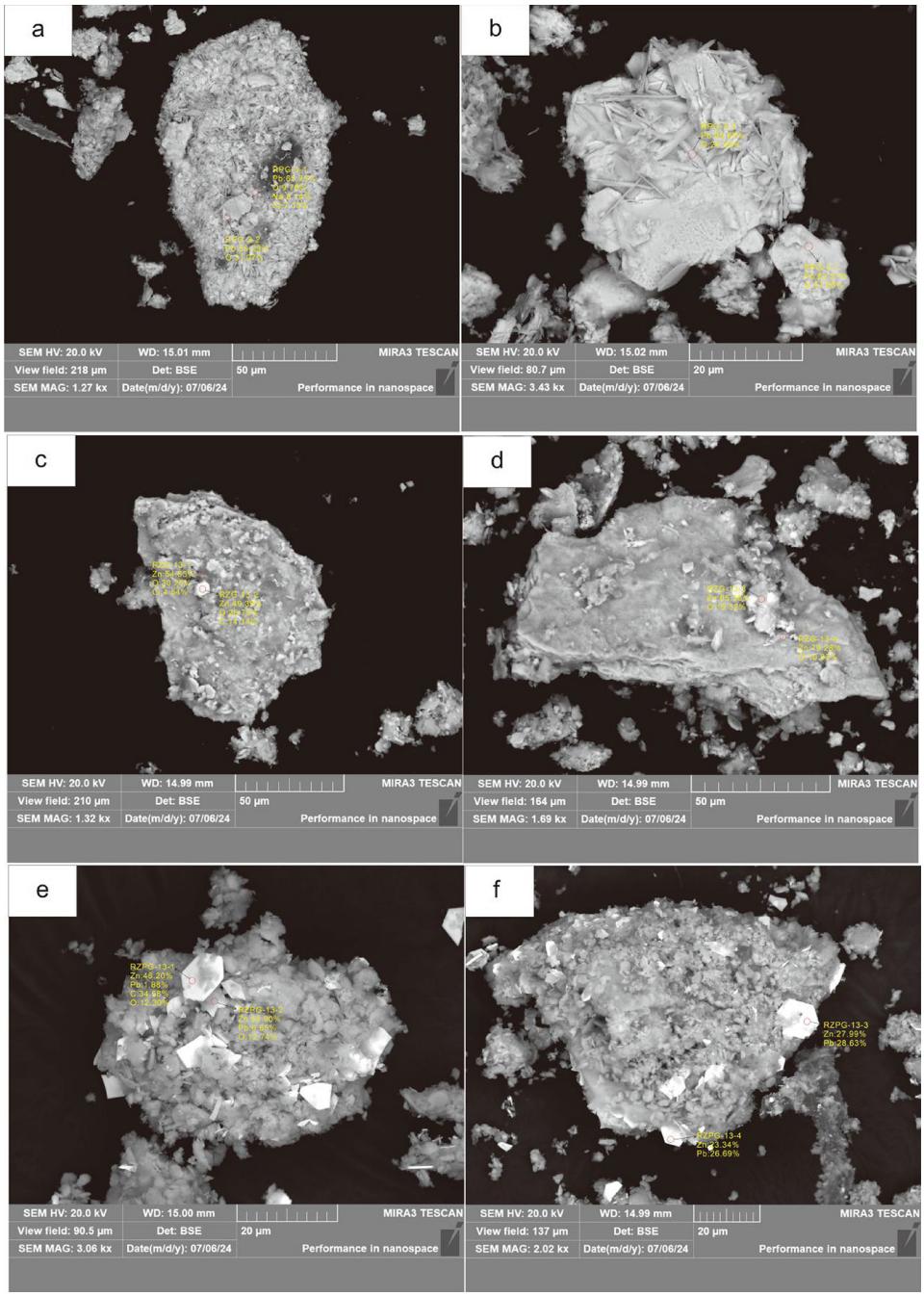

Fig. 7 Electron microscope images of the hydrolysis products from the Pb-Zn-NaCl-H_2O system: (**a**) and (**b**) localized scanning images of hydrolysis samples from Experiment 2; (**c**) and (**d**) localized scanning images of hydrolysis products from Experiment 4; (**e**) and (**f**) localized scanning images of hydrolysis products from Experiment 6

irregular block-like aggregates, with morphological characteristics similar to those observed in the Pb-NaCl-H_2O system. The individual crystal particles were of moderate size (Fig. 7e, f) and displayed a diverse range of shapes, including granular, elongated, and flaky forms. The primary constituents were lead and zinc hydroxides, accompanied by minor carbonate components (Table 2). Taking the RZPG-13 sample as an example, PbO and ZnO are the primary constituents. The relative proportions of Pb and Zn elements show spatial variability, with Zn being predominant in most regions. Elemental analysis was conducted at selected points along the edges, revealing that Pb constitutes 28.63%, Zn 27.99%, and O 15.01%.

Notably, carbon (C) constitutes a significant proportion in all three systems, suggesting the presence of carbonate components in the products. The precise mineral types will be identified through subsequent physical phase analysis. Given that the solution employed was sodium chloride (NaCl), despite thorough rinsing, trace amounts of Na and Cl elements remained in the precipitate.

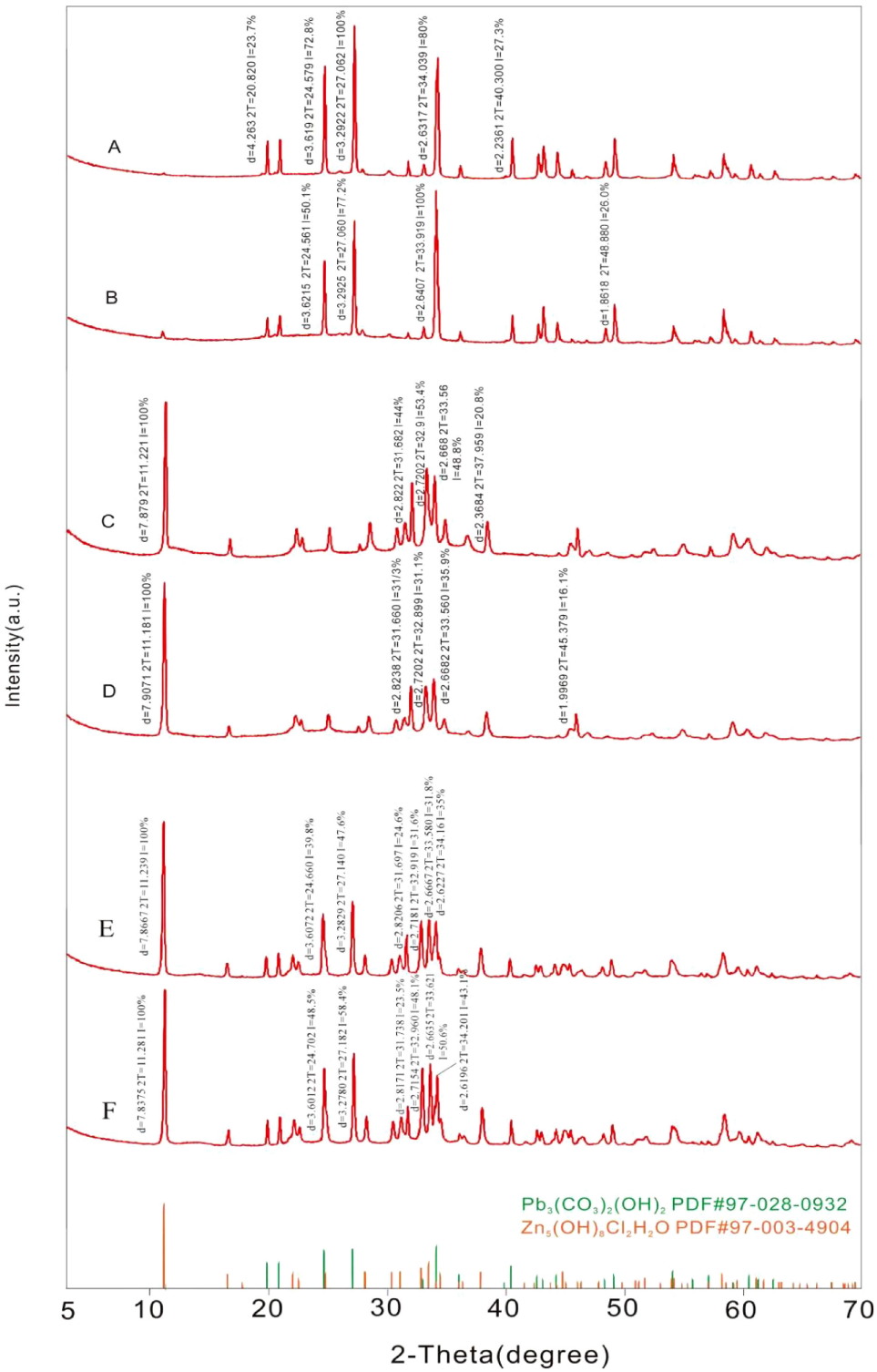

Fig. 8 XRD diffractogram: XRD diffraction patterns of the isolated water phase (**A**) and the retained water phase (**B**) in the Pb-NaCl-H_2O system; XRD diffraction patterns of the isolated water phase (**C**) and the retained water phase (**D**) in the Zn-NaCl-H_2O system XRD diffraction patterns of the isolated water phase (**E**) and the retained water phase (**F**) in the Pb-Zn-NaCl-H_2O system

3.3.3 XRD test results

Comparing the diffractograms of the precipitate samples from the two experimental groups showed that there is no significant difference in the angular distribution of the main peaks. This observation indicates that the variations in crystal morphology and the primary mineral compositions between the samples are minimal. However, the diffraction intensity of the isolated water group in this system is marginally lower than that of the retained water group. Conversely, the half-height width of the isolated water group is notably higher. This suggests that, within the Pb and Zn-NaCl-H_2O

system, the crystals of the isolated water group generally exhibit larger grain sizes and higher numbers than those of the retained water group.

As shown by the results of the physical phase analysis (Table 3) and the XRD diffraction pattern (Fig. 8E, F), the primary mineral constituents in the precipitated samples of the Pb, Zn-NaCl-H_2O system are simonkolleite [$Zn_5(OH)_8Cl_2H_2O$] and hydrocerussite [$Pb_3(CO_3)_2(OH)_2$]. These findings align with those observed in the single-metal systems. The content of simonkolleite is approximately between 50% and 60%, while the hydrocerussite is around 20%. The ratio of Pb to Zn precipitates is close to 6:2 in both reaction groups. However, compared to the Pb-NaCl-H_2O and Zn-NaCl-H_2O systems, this system exhibits more complex mineral phases. The oxides of Pb and Zn range from 4% to 7%, and the carbonate products range from 2.5% to 9.6%, with significantly higher levels of Zn than Pb.

4 Discussion

4.1 Effect of different systems on the hydrolysis reaction of Pb and Zn

Combining the results from various sets of experimental tests, it is evident that the hydrolysis products of Zn exhibit a higher re-solubility compared to Pb in both systems. This characteristic is largely unaffected by whether the hydrolysis products remain in contact with the solution post-hydrolysis. This observation is reflected in the significant disparity in metal ion precipitation rates observed between Zn and Pb in the solution sample tests. Compared with the Pb-NaCl-H_2O and Zn-NaCl-H_2O systems, the Pb and Zn ions in the Pb-Zn-NaCl-H_2O system exhibit varying degrees of inhibition over time, with lead ions being significantly more affected than zinc ions. In the Pb-NaCl-H_2O system, lead ions demonstrate a consistently high degree of hydrolysis that remains largely unaffected by temporal changes or post-hydrolysis conditions, which can be considered negligible. However, in the Pb and Zn-NaCl-H_2O system, the situation changed markedly, with the precipitation rate decreasing from over 99%–64.8%. The loss of hydrolysis products became particularly pronounced, especially when the hydrolyzed material remained in contact with the solution post-hydrolysis.

Combined with previous studies (Zhang et al. 2016; Wang et al. 1995) and the analysis of test results, the following may be the reasons.

(1) In the Pb-Zn-NaCl-H_2O system, the presence of two metal ions under identical environmental conditions induces a common ion effect. During the reaction, distinct metal cations compete for H^+ ions in the environment, ultimately leading to a reduced degree of hydrolysis for both ions;

(2) With the passage of time, the quantity of hydrolysis products of Pb and Zn ions diminishes to a certain extent. Prolonged exposure to retained water exacerbates this loss, and the "re-dissolution phenomenon" may be the primary factor contributing to this outcome. After hydrolysis, prolonged contact between the hydrolysis products and the solution will facilitate the reverse reaction, leading to a certain degree of re-dissolution of the hydrolysis products. Furthermore, as a reversible chemical reaction, the hydrolysis reaction's equilibrium constant is a crucial parameter in determining its final extent. In a fluid environment, hydroxide ions play a predominant role. Based on the balanced Eq. (5) for the hydrolysis reactions of Pb and Zn, a higher concentration of hydroxide ions coupled with a smaller K value indicates a less favorable reaction, resulting in a lower degree of reaction completion. The hydrolysis process generates acidic products. After the reaction has proceeded to completion, the hydrolysis products remain in a weakly alkaline environment. Therefore, the concentration of hydrogen ions in this environment gradually increases. Compared with isolated water molecules, the system will tend to favor the reverse reaction, which consumes hydrogen ions. In conjunction with the influence of temporal factors, the quantity of ultimately retained hydrolyzed products progressively diminishes. This observation aligns with prior verification that lower temperatures result in reduced acidity and a shorter duration for irreversible hydrolysis reactions. (Wang et al. 1995; Knauss et al. 2001). Based on the metal-ion-rich acidic solutions configured in prior studies, the concentration of Zn ions in the Zn-NaCl-H_2O system is significantly higher than that of Pb ions in the Pb-NaCl-H_2O system. According to Le Chatelier's principle, any change in a condition affecting equilibrium will result in a shift of the equilibrium in a direction that tends to counteract this change.

4.2 Morphological characterization and mineral composition of Pb and Zn hydrolysis product

Currently, researchers have proposed a preservation mechanism for the crystal orientation of reactants: when the product and reactant exhibit a matching epitaxial adhesion relationship during the dissolution-reprecipitation process, the supersaturation threshold of the product can be reduced. This change in growth mechanism to two-dimensional nucleation facilitates uniform lamellar growth of the product on the reactant, thereby promoting the transfer and preservation of crystallographic information (Putnis

2009; Brugger et al. 2010; Ruiz-Agudo et al. 2014). This understanding necessitates further substantiation through systematic micro- and nanoscale mineral lattice investigations (Li et al. 2024). The carbonate mineral-fluid reaction proceeds as a progressive, stage-like process of dissolution and reprecipitation, transitioning from a state of disequilibrium to equilibrium. This transition should be effectively characterized by surface microzonation and compositional zonation studies. In this experiment, scanning electron microscopy was employed to capture images of the hydrolysis products, thereby acquiring essential information regarding the crystal morphology of these products. This data will facilitate a more accurate reconstruction of the Pb and Zn hydrolysis processes.

Based on the BSE images of hydrolysis products obtained under various systems, the crystal sizes of the precipitates generated under different conditions generally range from 40 to 120 μm in length and from 25 to 60 μm in width. Notably, there are significant differences in the crystal morphology of minerals corresponding to different metal elements.

In the Pb-NaCl-H_2O system, hydrocerussite [$Pb_3(CO_3)_2(OH)_2$] exhibits small grain sizes with non-uniform morphology. Most grains display unidirectional elongation and agglomeration, featuring uneven surfaces with localized granular regions and incomplete structures. The distribution of mineral compositions is heterogeneous. However, under crystalline conditions, a few crystals develop into acicular and fibrous forms, showing more uniform mineral compositions and a significant enhancement in effective mineral content. Given the limited number of crystallographic studies on hydrocerussite, we utilize white cerussite, which has a similar composition, for comparative analysis. In nature, cerussite typically occurs as a secondary oxidation mineral of galena. Its single crystals are commonly observed in short columnar and conical forms, while its aggregates develop into dense masses, stalactites, and nodules (Bai 2017). Comparing the crystal characteristics of the precipitates obtained in this experiment (Fig. 6a, b), they exhibit a close match in grain size and crystal morphology. However, notably, laboratory conditions are significantly different from the natural mineral growth environment. Therefore, the aggregate form does not exhibit more pronounced nodule- or earth-like morphologies. However, its primary mineral composition is $Pb_3(CO_3)_2(OH)_2$, accompanied by significant amounts of lead carbonates and oxides. Despite this, its characteristics remain highly consistent with the formation mechanism of cerusite.

Compared to the Zn-NaCl-H_2O system, the grain size of simonkolleite [$Zn_5(OH)_8Cl_2H_2O$] in the Pb-NaCl-H_2O system is notably larger. The morphology exhibits a more uniform structure, predominantly characterized by two-dimensional extension with smooth and elongated features. This results in the development of sheet- and plate-like crystals, displaying a clear hierarchical organization. The mineral composition is evenly distributed, and the crystal forms are well defined. Notably, the carbonate composition in this system has been significantly reduced compared to the Pb-NaCl-H_2O system, which aligns with the findings from the physical phase analysis. In natural settings, hydrozincite commonly occurs in the oxidized zones of Zn-rich veins and is categorized among common secondary carbonates such as hydrocerussite. Hydrozincite crystals typically manifest as thin strips or flakes, rarely forming large crystals. The overall morphology is characterized by flattened or elongated slabs, while the aggregate form is predominantly massive and dense (Zhao 2017). The crystal characteristics of the zinc chlorate ore obtained from the contrast experiment (Fig. 6c, d) exhibit fundamental consistency in terms of crystal morphology. Given that the precipitate is composed of various oxides and hydroxides, the crystal size is marginally larger than those formed under natural conditions.

The morphology of the mixture of hydrozincite, $Zn_5(OH)_8Cl_2H_2O$, and hydrocerussite, $Pb_3(CO_3)_2(OH)_2$, in the Pb-Zn-NaCl-H_2O system exhibits distinctive characteristics. Unlike the two aforementioned systems, the grain size distribution in this system is non-uniform, intermediate between the other two systems. The crystal morphology closely resembles that observed in the Pb-NaCl-H_2O system, with some regions developing a scale-like crystalline pattern while most areas exhibit granular structures. The surface texture is uneven, yet the overall crystal growth remains unidirectionally extended, albeit with more complete crystal forms. The mineral composition is predominantly characterized by Zn ions, which account for 50%–70% in most regions. Pb ions range from 3% to 29%, except in the marginal flaky highlighted areas where carbonate minerals are also significant and Pb ions are predominant. The similarities and differences between the natural crystals of simonkolleite and hydrocerussite, as well as those obtained experimentally, have been thoroughly examined in the discussion of the first two systems and will not be reiterated here.

In summary, the crystal growth of hydrolysis products under various systems generally adheres to a specific pattern. Specifically, Pb oxide crystals exhibit smaller dimensions with an irregular surface and unidirectional elongation. In contrast, Zn oxide crystals are characterized by larger dimensions, well-defined morphology, and bidirectional extension. In the Pb-Zn-NaCl-H_2O system, the Pb-Zn hydroxide crystals exhibit characteristics of crystal forms intermediate between those of lead and zinc hydroxides, with grain sizes also falling within this intermediate range. Moreover, the distribution of mineral components is notably heterogeneous.

4.3 Dynamic processes and geological significance of hydrolysis reactions of Pb and Zn

The Pb-Zn hydrolysis reaction in this experiment was conducted by introducing an appropriate concentration of alkaline solution into the metal-rich acidic solution. This facilitated the transformation of Pb and Zn ions from their chloro-complex state, which is characterized by extensive and long-distance migration, to an insoluble oxide state that is more stable and easier to preserve. The objective was to simulate the initial metal precipitation stage of Pb-Zn deposit formation, specifically the geological process where metal-ion-rich acidic fluids enter the ore-hosting space primarily composed of carbonate rocks under the influence of tectonic stress. It is intended to simulate the initial metal unloading stage of the mineralization process, the acidic fluid containing a large number of metal ions entering the carbonate rock-based ore-holding space under tectonic stress.

From the T-lgK and P-lgK phase diagrams (Fig. 9) of the complexes, it is evident that the stability of the chlorine complexes of Pb and Zn is significantly higher at high temperatures compared to low temperatures. Consequently, the chlorine complexes of Pb and Zn, which are stable under room temperature and normal pressure conditions, are expected to exhibit enhanced stability in high-temperature and -pressure environments. Moreover, the stability of the chlorine complexes under the metallogenic temperature and pressure conditions of HZT-type deposits shows relatively minor variations. Therefore, despite the discrepancy between the actual geological evolution and the ambient temperature and pressure conditions of this experiment, the conclusions derived from the experiment remain equally applicable to this type of deposit within the range of mineralization temperatures and pressures.

Based on the results of the physical phase analysis obtained (Table 3) and the results of previous research (Zhang et al 2016; Yang et al. 1999; Liu et al 1984), the following inferences are made about the chemical dynamic processes of the two main hydrolysis products of Pb and Zn:

Under medium-alkaline and high ionic activity conditions, a significant quantity of metal ions, present as chloride complexes, undergo rapid stepwise hydrolysis, releasing hydrogen ions (see reaction formulae 1–4). Consequently, Pb and Zn precipitate as hydroxides and oxides. To simulate the actual geological mineralization process more accurately, the experiment was conducted in an open system. This allowed atmospheric CO_2 to dissolve in the solution, forming carbonate ions (Eq. 6), which subsequently reacted with both the pre-formed Pb and Zn hydrolysis products and the remaining Pb and Zn ions (Eqs. 7–8), leading to the formation of Pb and Zn carbonate minerals. With the combined influence of carbonate ions (the predominant factor) and hydroxide ions in solution, lead carbonate will progressively transform into basic lead carbonate (Eq. 9) over an extended period (Dong 2012). In the presence of a high concentration of chloride ions in solution, the hydrolysis reaction proceeds, causing the solution to become acidic. Zinc carbonate is consequently transformed into hydrozincite (Eq. 10). Over time, hydrozincite in an acidic environment will convert into simonkolleite via reaction (Eq. 11). Additionally, any remaining zinc oxide in the solution reacts with the resulting zinc chloride to further produce simonkolleite (Eq. 12).

$$CO_2 + H_2O \Leftrightarrow H_2CO_3 \tag{6}$$

$$CO_3^{2-} + Pb^{2+} \Leftrightarrow PbCO_3 \tag{7}$$

$$CO_3^{2-} + Zn^{2+} \Leftrightarrow ZnCO_3 \tag{8}$$

$$2CO_3^{2-} + 3Pb^{+} + 2OH^{-} \Leftrightarrow Pb_3\left(CO_3\right)_2(OH)_2 \tag{9}$$

$$5ZnCO_3 + 6H^{+} + 3CO_3^{2-} \rightarrow Zn_5\left(CO_3\right)_2(OH)_6 + 6CO_2\uparrow \tag{10}$$

$$2\left[ZnCO_3 \cdot Zn_2(OH)_4 \cdot H_2O\right] + 4HCl + H_2O \rightarrow Zn_5(OH)8Cl_2H_2O + ZnCl_2 + 4H_2O + 2CO_2\uparrow \tag{11}$$

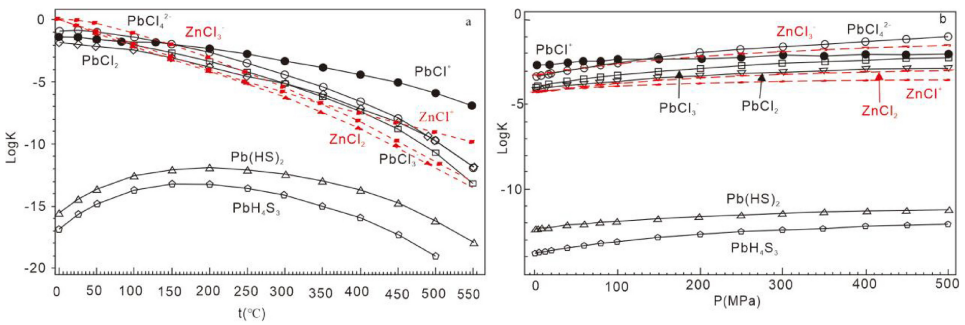

Fig. 9 Effect of temperature pressure on complex stability (modified from Reed 2006). **a** t-lg K plot for complexes ($P = 80.00$ MPa); **b** P-lg K plot for complexes ($t = 200$ °C), as referenced by Zhang et al. (2019a, b)

$$ZnCl_2 + 4ZnO + 5H_2O \rightarrow Zn_5(OH)8Cl_2H_2O \quad (12)$$

The experimental results demonstrate that the duration required for hydrolysis to achieve complete metal unloading is relatively brief. As a semi-enclosed environment, the ore-hosting space possesses the capacity to retain a sufficient volume of fluid, thereby ensuring the hydrolysis reaction proceeds to completion. By comparing the two experimental groups, it was found that despite a certain degree of re-dissolution occurring post-hydrolysis, the preserved precipitates still maintain a very high effective mineral content. This condition is conducive to storing a large quantity of metal precipitates. Therefore, hydrolysis isolation in a single-metal system has greater significance for retaining metal precipitates. The hydrolysis products of Pb and Zn exhibit distinct crystallization patterns in various systems. Zn hydroxide crystals display a more complete morphology and retain a higher hydroxide content compared to Pb hydroxide. In mixed systems, Zn hydrolysis products are predominant; however, the presence of Pb significantly influences the morphology of the resulting crystals.

5 Conclusion

The synthesis of the above experimental data and analysis results on the dynamic process of Pb and Zn hydrolysis under different systems yielded the following conclusions:

(1) In the hydrolysis processes of different systems, significant variations are observed in both the hydrolysis behavior and influencing factors. For single-metal systems, the impact of time on Pb ion hydrolysis is minimal, whereas Zn ions exhibit a clear trend of decreasing solubility over time. This suggests that the hydrolysis products of Zn are more prone to re-dissolution compared to those of Pb. In mixed systems, there is an observable inhibitory effect on the hydrolysis of both Pb and Zn ions. Specifically, Zn ions demonstrate a stronger tendency for hydrolysis relative to Pb ions.

(2) The hydrolysis products of Pb and Zn primarily consist of hydroxide precipitates with carbonate components. The mineral composition and crystallization characteristics of the hydrolysis products from different metal ions show certain variations. Specifically, in the Pb-NaCl-H_2O system, the hydrolysis products feature finer grains, predominantly agglomerated crystal structures, uneven crystal surfaces, unidirectional crystal growth, and a significant proportion of carbonate in the mineral composition. The hydrolysis products of the Zn-NaCl-H_2O system exhibit larger grain sizes, with crystal morphology predominantly characterized by acicular and fibrous structures. The hydrolysis products of the Pb, Zn-NaCl-H_2O system exhibit crystalline characteristics consistent with both Pb and Zn hydroxides. Apart from the highly bright regions at the particle edges, most of the crystal structure demonstrates a Pb to Zn hydroxide ratio of approximately 2:7, which aligns well with the findings from phase analysis.

(3) The hydrolysis products of Pb and Zn maintained a high effective mineral composition across all systems. However, the homoionic effect observed in the Pb and Zn-NaCl-H_2O systems had a more significant impact on the hydrolysis of Pb ions. In contrast, the isolation of the fluid environment following the completion of hydrolysis is more conducive to the preservation of hydrolysis products, thereby minimizing the extent of re-dissolution that may occur over time in this environment. The hydrolysis products mainly go through three stages of oxides/hydroxides → carbonates → alkali carbonates. Ultimately, the precipitates of the three mineral forms will coexist; however, the alkali carbonate precipitates will dominate. In the Pb–Zn-NaCl-H_2O system, the ratio of Zn and Pb alkali carbonate products is 6:2.

Acknowledgements This work was financed jointly by National Natural Science Foundation of China (42472127, 42172086), the Yunnan Major Science and Technological Projects (202202AG050014–01), Yunnan Province Basic Research Key Program (202401BN070001-002), (Yunnan Mineral Resources Prediction and Evaluation Engineering Laboratory (2011), and Yunnan Provincial Geological Process and Mineral Resources Innovation Team (2012).

Author contributions Junfeng Liu: carried out the experiment, data curation, formal analysis, investigation, writing—original draft, writing—review and editing; Yan Zhang: funding acquisition, project administration, writing—review and editing; Runsheng Han: funding acquisition, project administration, writing—review and editing; Pingtang Wei: conceptualization, project administration, writing—review and editing; Wei Zhu: preparation of scheme documentation, sample processing procedures, investigation.

Funding This work was financed jointly by the National Natural Science Foundation of China (42472127, 42172086) the Yunnan Major Science and Technological Projects (202202AG050014), the Yunnan Major Project of Basic Research (202401BN070001-002), Yunnan Mineral Resources Prediction and Evaluation Engineering Research Center (2011), Innovation Team Program of Kunming University of Science and Technology, Yunnan Province.

Declarations

Conflict of interest The authors declare that they have no known competing financial interests or personal relationships that could have appeared to influence the work reported in this paper.

References

Anderson GM (1973) The hydrothermal transport and deposition of galena and sphalerite near 100 °C. Econ Geol 68(4):480–492. https://doi.org/10.2113/gsecongeo.68.4.480

Anderson GM (1975) Precipitation of Mississippi valley-type ores. Econ Geol 70(5):937–942. https://doi.org/10.2113/gsecongeo.70.5.937

Bai X (2017) Study on sulfide flotation and mechanism of Pb cerussite. Kunming Uni Tech

Bodnar RJ, Lecumberri-Sanchez P, Moncada D, Steele-MacInnis M (2014) 13.5–fluid inclusions in hydrothermal ore deposits. Treatise Geochem 13:119–142. https://doi.org/10.1016/B978-0-08-095975-7.01105-0

Brugger J, McFadden A, Lenehan CE, Etschmann B, Xia F, Zhao J, Pring A (2010) A novel route for the synthesis of mesoporous and low-thermal stability materials by coupled dissolution-reprecipitation reactions: Mimicking hydrothermal mineral formation. Chimia 64(10):693–698. https://doi.org/10.2533/chimia.2010.693

Caciagli NC, Manning CE (2003) The solubility of calcite in water at 6–16 kbar and 500–800 °C. Contrib Mineral Petrol 146(3):275–285. https://doi.org/10.1007/s00410-003-0501-y

Carpenter AB, Trout ML, Pickett EE (1974) Preliminary report on the origin and chemical evolution of lead-and zinc-rich oil field brines in central Mississippi. Econ Geol 69(8):1191–1206. https://doi.org/10.2113/gsecongeo.69.8.1191

Chen X, Liu JJ, Zhang DH, Tao YL (2014) A review of the migration and precipitation mechanism of Zn in hydrothermal deposits. Geological J China Uni 20(03):388–406

Chen X, Liu JJ, Li YC, Wang YL, Zhang DH, Tao YL, Cao Q (2015) A review of studies on the migration and precipitation mechanism of Pb in hydrothermal deposits. Bull Geol Sci Tech 34(03):45–57

Dean JA (1991) Thermodynamic property. Lange's handbook of chemistry. Science Press, Beijing, pp 1467–1638

Dong CS, Li JZ, Sun ZX (2012) Synthesis and conversion of Pb carbonate and alkaline Pb carbonate. J Jinan Uni (Natural Sci Ed) 26(01):73–77. https://doi.org/10.3969/j.issn.1671-3559.2012.01.016

He JJ, Ding X, Wang YR, Sun WD (2015) The effects of precipitation-aging-re-dissolution and pressure on hydrolysis of fluorine-rich titanium complexes in hydrothermal fluids and its geological implications. Acta Petrol Sin 31(7):1870–1878

Helgeson HC (1964) Complexing and hydrothermal ore deposition. MacMillan New York

Knauss KG, Dibley MJ, Bourcier WL, Shaw HF (2001) Ti(IV) hydrolysis constants derived from rutile solubility measurements made from 100 to 300 °C. Appl Geochem 16(9–10):1115–1128. https://doi.org/10.1016/S0883-2927(00)00081-0

Li FJ, Qi YQ, Haotian BOW (2024) A review of studies on mineral dissolution and reprecipitation processes. Bull Mineral Rock Geochem 43(01):240–258. https://doi.org/10.19658/j.issn.1007-2802.2023.42.118

Liu YJ et al (1984) Platinum group element. Elemental geochemistry. Science Press, Beijing, pp 343–359

Liu YZ, Wang EJ, Wang SR, Guo GJ, Li DP, Zhang BL (2018) Water-rock interaction in Jiaojia gold deposits and variations of the ore-forming fluid. Geol J China Univ 24(6):907–917. https://doi.org/10.16108/j.issn1006-7493.2018036

Liu WH, Spinks SC, Glenn M, MacRae C, Pearce MA (2021) How carbonate dissolution facilitates sediment-hosted Zn-Pb mineralization. Geology 49(11):1363–1368. https://doi.org/10.1130/g49056.1

Matthews A, Katz A (1977) Oxygen isotope fractionation during the dolomitization of calcium carbonate. Geochim Cosmochim Acta 41(10):1431–1438. https://doi.org/10.1016/0016-7037(77)90249-6

Mei Y, Sherman DM, Liu WH, Etschmann B, Testemale D, Brugger J (2015) Zinc complexation in chloride-rich hydrothermal fluids (25–600 ℃): a thermodynamic model derived from *ab initio* molecular dynamics. Geochim Cosmochim Acta 150:265–284. https://doi.org/10.1016/j.gca.2014.09.023

Mesmer RE, Baes Jr CF (1976) The hydrolysis of cations. New York, pp 936–938.

Putnis A (2009) Mineral replacement reactions. Rev Mineral Geochem 70(1):87–124. https://doi.org/10.2138/rmg.2009.70.3

Reed MH (2006) Sulfide mineral precipitation from hydrothermal fluids. Rev Mineral Geochem 61(1):609–631. https://doi.org/10.2138/rmg.2006.61.11

Roedder E, Bodnar RJ (1997) Fluid inclusion studies of hydrothermal ore deposits. In: Barnes HL (ed) Geochemistry of hydrothermal ore deposits, 3rd edn. Wiley, New York, pp 657–698

Ruiz-Agudo E, Putnis CV, Putnis A (2014) Coupled dissolution and precipitation at mineral–fluid interfaces. Chem Geol 383:132–146. https://doi.org/10.1016/j.chemgeo.2014.06.007

Stoffell B, Appold MS, Wilkinson JJ, McClean NA, Jeffries TE (2008) Geochemistry and evolution of Mississippi valley-type mineralizing brines from the tri-state and northern Arkansas districts determined by LA-ICP-MS microanalysis of fluid inclusions. Econ Geol 103(7):1411–1435. https://doi.org/10.2113/gsecongeo.103.7.1411

Touret JLR (2001) Fluids in metamorphic rocks. Lithos 55(1–4):1–25. https://doi.org/10.1016/S0024-4937(00)00036-0

Van Baalen MR (1993) Titanium mobility in metamorphic systems: a review. Chem Geol 110(1–3):233–249. https://doi.org/10.1016/0009-2541(93)90256-i

Wang YR, Chen WH, Zhang HX (1995) Experimental study on the irreversible reaction of high-temperature hydrolysis of Sn, Nb and Ta fluorine complexes. Geochemistry S1:183–190

Wang WQ, Qi FC, Lin WJ, Zhang YY, Xiu XQ (2019) Experimental study on temperature and pressure constraints of uranium dissolution in the sodium bicarbonate solution. World Nucl Geosci 36(3):133–139

Wilkinson JJ, Stoffell B, Wilkinson CC, Jeffries TE, Appold MS (2009) Anomalously metal-rich fluids form hydrothermal ore deposits. Science 323(5915):764–767. https://doi.org/10.1126/science.1164436

Yan HB, Ding X, Wang Y, Mi M, Sun WD (2020) Fluid activity of platinum group elements. Acta Petrol Sin 36(01):85–98. https://doi.org/10.18654/1000-0569/2020.01.10

Yang YR (1999) Physicochemical properties and significance of supercritical water. Trends and perspectives in fluid geoscience. Seismological Press, Beijing, pp 173–180

Yardley BWD (2005) 100th anniversary special paper: Metal concentrations in crustal fluids and their relationship to ore formation. Econ Geol 100(4):613–632. https://doi.org/10.2113/100.4.613

Yeh TZ (2014) Theory and method of prospecting prediction in the exploration area. In: Non-magmatic post-generation hydrothermal Pb-Zn deposits in carbonatite hosted ores, Beijing, pp 41–69

Zhang DH (1997) Review on the mechanism of metal precipitation in ore-forming fluids. Bull Geol Sci Technol 16(3):54–59

Zhang S, Liu YS (1995) Experimental study on gold solubility and its geological significance. Geochimica 24:168–176. https://doi.org/10.19700/j.0379-1726.1995.s1.021

Zhang Y, Han RS, Wei PT (2016) A review on the transport and precipitation mechanism of Pb and Zn elements in the ore-forming fluids of carbonatite-type Pb-Zn deposits. Geol Theory Eval 62(01):187–201

Zhang Y, Han RS, Ding X, He JJ, Wang YR (2019a) An experimental study on metal precipitation driven by fluid mixing: implications for genesis of carbonate-hosted lead–zinc ore deposits. Acta Geochim 38(2):202–215. https://doi.org/10.1007/s11631-019-00314-4

Zhang Y, Han RS, Ding X, Wang YR, Wei PT (2019b) Experimental study on fluid migration mechanism related to Pb–Zn superenrichment: implications for mineralisation mechanisms of the Pb–Zn deposits in the Sichuan–Yunnan–Guizhou. SW China Ore Geol Rev 114:103110. https://doi.org/10.1016/j.oregeorev.2019.103110

Zhang PF, Wang CJ, Qiu YB, Ni R, Zhao HZ, Chen Y (2025) Quantitative calculation model and application of sandstone secondary porosity based on mineral dissolution experiments. Rock Mineral Anal. https://doi.org/10.15898/j.ykcs.202404200091

Zhao SR (2017) Crystallography and mineralogy. Higher Education Press, Beijing

Zhao XL, Li HP, Su GL (2013) A progress on quartz solubility in aqueous fluids at high temperature and high pressure. Acta Mineral Sin 33(1):75–82. https://doi.org/10.16461/j.cnki.1000-4734.2013.01.011